JOURNAL OF combinatorial CHEMISTRY

Article

Combinatorial Electrochemical Synthesis and Characterization of Tungsten-Based Mixed-Metal Oxides

S. H. Baeck, T. F. Jaramillo, C. Brndli, and E. W. McFarland

J. Comb. Chem., **2002**, 4 (6), 563-568• DOI: 10.1021/cc020014w • Publication Date (Web): 07 September 2002

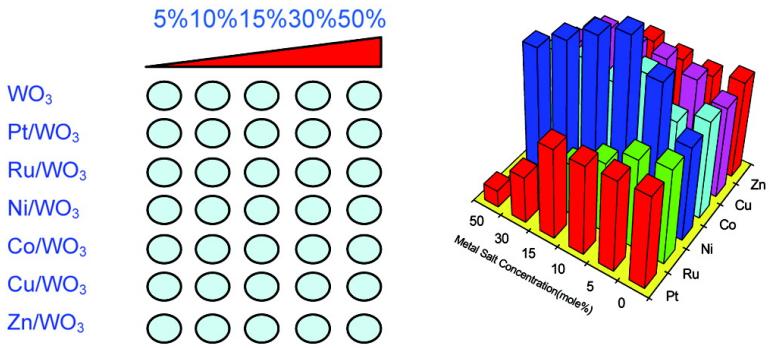

More About This Article

Additional resources and features associated with this article are available within the HTML version:

- Supporting Information
- Links to the 9 articles that cite this article, as of the time of this article download
- Access to high resolution figures
- Links to articles and content related to this article
- Copyright permission to reproduce figures and/or text from this article

View the Full Text HTML

Journal of Combinatorial Chemistry is published by the American Chemical Society.
1155 Sixteenth Street N.W., Washington, DC 20036

Combinatorial Electrochemical Synthesis and Characterization of Tungsten-Based Mixed-Metal Oxides

S. H. Baeck, T. F. Jaramillo, C. Brändli, and E. W. McFarland*

Department of Chemical Engineering, University of California−Santa Barbara, Santa Barbara, California 93106-5080

Received March 8, 2002

Automated systems for electrochemical synthesis and high-throughput screening of photoelectrochemical materials were developed and used to prepare tungsten-based mixed-metal oxides, $W_nO_mM_x$ [M = Ni, Co, Cu, Zn, Pt, Ru, Rh, Pd, and Ag], specifically for hydrogen production by photoelectrolysis of water. Two-dimensional arrays (libraries) of diverse metal oxides were synthesized by automated cathodic electrodeposition of the oxides on Ti foil substrates. Electrolytes for the mixed oxides were prepared from various metal salts added to a solution containing tungsten stabilized as a peroxo complex. Electrodeposition of the peroxo-stabilized cations gave rise to three distinguishable oxide groups: (1) mixed-metal oxides [Ni], (2) metal-doped tungsten oxides [Pt, Ru, Rh, Pd, Ag], and (3) metal−metal oxide composites [Co, Cu, Zn]. The oxides typically showed n-type semiconducting behavior. Automated measurement of photocurrent using a scanning photoelectrochemical cell showed the W−Ni mixed oxide had the largest relative zero bias photocurrent, particularly at a low Ni concentration (5−10 atomic percent Ni). Pt and Ru were also found to increase the photoactivity of bulk tungsten oxide at relatively low concentrations; however, at concentrations above 5 atomic percent, crystallization of WO_3 was inhibited and photoactivity was diminished. Addition of Co, Cu, and Zn to WO_3 was not found to improve the photoelectrochemical activity.

1. Introduction

Tungsten oxide (WO_3) is an indirect bandgap semiconductor with interesting photoconducting behavior. It is presently used in electrochromic devices and chemical sensors and is a potentially low-cost material for solar energy applications.[1−4] WO_3, with numerous crystal structures, has been prepared by a variety of physical and chemical methods.[5,6] Electrochemical deposition methods have been used for WO_3 deposition by dissolving Na_2WO_4 in sulfuric acid[7,8] or tungsten powder in hydrogen peroxide.[9,10] The electrodeposition method has many advantages over other synthesis routes in terms of economics and flexibility for making large surface area films. The low conductivity of tungsten oxide has limited its application in photovoltaic devices; however, efforts to improve the properties using dopants such as Ni and Co have shown promise.[11,12] Progress, however, has been slow, and there is limited theoretical basis for selecting dopants or dopant concentrations.

Automated electrochemical synthesis and screening using combinatorial methodologies have been shown to increase the rate of investigation of the effects of composition and structure on materials performance. Combinatorial chemistry is the deliberate synthesis and screening of very large numbers of diverse new materials from different combinations of specific building block atoms and molecules.[13−15] Applied to functional inorganic materials, these methods have been used to rapidly investigate large numbers of mixed-metal oxides as potential phosphors, catalysts, dielectric materials,[16−18] and inorganic supports.[19] The versatility of electrochemical methods has been applied to catalyst screening and synthesis.[20] Automated electrochemical methods for creating and screening collections of compositionally or structurally varied materials (libraries) for photoelectrochemical performance have recently been described.[21,22] Electrochemical methods lend themselves well to the combinatorial synthesis of inorganic materials because of the many synthesis variables under direct control such as voltage, current density, and electrolyte, which can be varied in a deliberate manner, resulting in great diversity of structure and composition. We used methods of automated electrochemical synthesis and screening to address the following questions: (1) Can combinatorial libraries of diverse metal-doped tungsten oxides be rapidly synthesized and screened electrochemically as potential photovoltaic and photoelectrochemical materials? (2) What are the photoelectrochemical functional effects of the compositional changes? (3) Can the photocatalytic properties of tungsten oxide be improved by doping? (4) Are there trends in photoelectrochemical performance as a function of composition that might improve our understanding of composition−function relationships?

2. Experimental Section

Tungsten cations were stabilized as peroxo complexes in an electrolyte prepared by dissolving 1.8 g of tungsten powder in 60 mL of 30% hydrogen peroxide solution. The excess hydrogen peroxide was subsequently decomposed with platinum black. The solution was diluted to 50 mM with a 50:50 mixture of water and 2-propanol. Additional

10.1021/cc020014w CCC: $22.00
Published on Web 09/07/2002

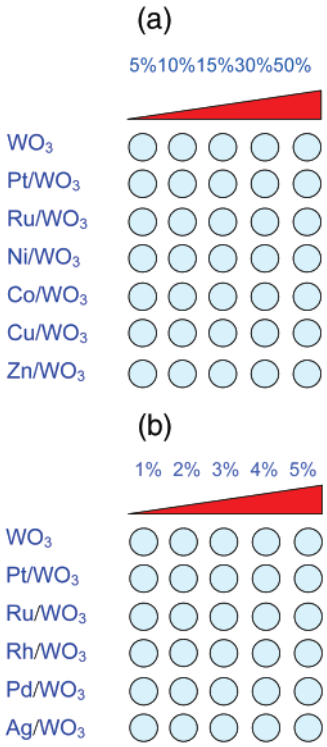

Figure 1. Library designs for (a) library A and (b) library B. The individual electrolyte contained peroxo-stabilized tungsten with metal salts added at the individual mole percentage for diversity.

metal species were introduced by adding different volumes of 50 mM metal chloride solutions to the tungstenperoxo solution. Library synthesis was performed on titanium foil substrates that were cleaned with aqueous detergent, acetone, and 2-propanol.

The films were deposited cathodically under potentiostatic control in an assembly of individual cells that formed an array. In brief, the assembly consisted of a polypropylene block 30 mm in thickness with 63−10.8 mm diameter holes. Each cell had an O-ring for sealing against the substrate. The block was affixed to the titanium foil substrate, forming up to 63 independent working electrodes. For maximum control of electrochemical synthesis, we developed a scanning electrode probe containing a platinum reference electrode and a platinum counter electrode. After the individual cells were filled with various electrolytes, the electrodes are scanned under computer control to each electrolytic well. Different structures and compositions of the oxides are electrodeposited in each well by varying the electrolyte composition and voltage across the library.

The library design shown in Figure 1a represents a 5 × 7 array of tungsten-based oxides (library A), with diversity achieved by variations in dopant species and metal chloride concentration. The library was deposited on titanium foil using the parallel reactor block. All wells except for the first row contained a mixture of tungstenperoxo electrolyte and metal salt. The first row served as a control and contained no added metal salts. Six metal chlorides were used in library A: Pt, Ru, Ni, Co, Cu, and Zn. The concentration of each species was varied from 5 to 50 mol %, and all films were deposited for 5 min at −1.0 V vs Pt reference electrode. After deposition, the library was calcined at 600 °C for 6 h in air.

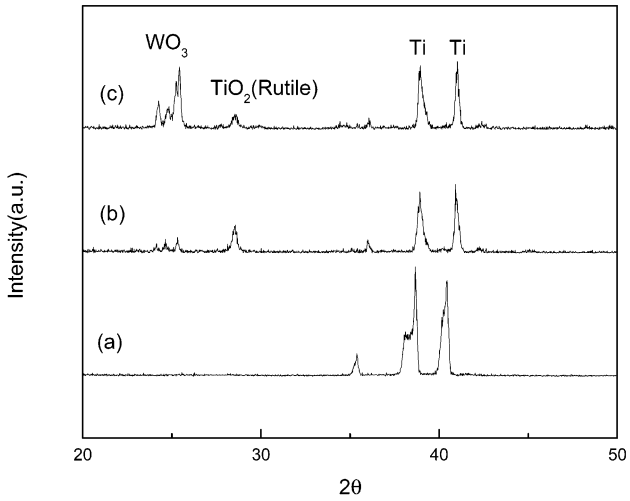

Figure 2. X-ray diffraction patterns of tungsten oxides on Ti foil: (a) as-synthesized calcined in air at (b) 400 °C and (c) 600 °C.

A library consisting of tungsten oxide with added Pt, Ru, Rh, Pd, and Ag was also synthesized (library B). All wells except for the first control row contained a mixture of tungsten and noble metals (Figure 1b). The concentrations of noble metals in the electrolytes were varied from 1 to 5 mol % with deposition for 5 min at −1.0 V vs Pt reference electrode. After deposition, the library was calcined at 600 °C for 6 h in air.

Library screening for photoelectrochemical activity was performed by measurement of photocurrent at 0 and 1 V bias. A scanning electrochemical probe, which is described in detail elsewhere, was used.[22] Under computer software control, the probe is translated to each library location and lowered onto the film, forming an O-ring seal. The probe contains a Pt working electrode and a Pt reference electrode connected to an EG&E 273A potentiostat. Sodium acetate (0.1 M) electrolyte is pumped automatically into the probe, and current−voltage data are obtained while the area is illuminated with a chopped light source. The source was an Oriel Xe 150 W lamp coupled by an optical fiber to the scanning probe with a measured output at the sample of 2.25 mW/cm^2. The current is monitored and stored throughout the voltage ramp cycle (0.01 V/s voltage ramp).

Selected library samples underwent more detailed quantitative analysis. Scanning electron microscopy (Philips, XL-30 ESEM-FEG) and electron stimulated energy dispersed X-ray spectroscopy (Princeton Gamma Tech, IMIX) were performed to determine surface morphology and composition. X-ray diffraction (Scintag, X2) was used to examine the crystal structures.

3. Results and Discussion

The as-deposited tungsten oxide control films (after drying at room temperature) were confirmed to be amorphous (Figure 2a). The film crystallized at 400 °C (Figure 2b), and XRD patterns were obtained from the film annealed at 600 °C consisting of highly crystalline tungsten oxide (Figure 2c). X-ray diffraction was conducted on samples from library A synthesized from the electrolyte with 15% dopant concentration (4th column in library A). For nickel, a mixed

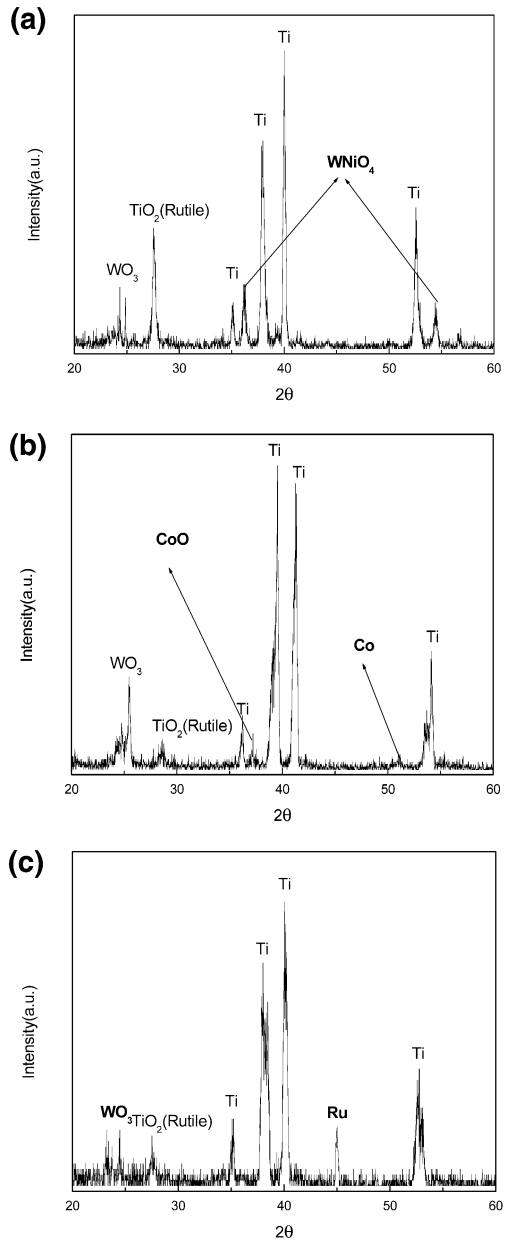

Figure 3. XRD patterns of (a) Ni-doped WO_3, (b) Co-doped WO_3, and (c) Ru-doped WO_3 synthesized from electrolyte with concentration of 15% of each dopant.

oxide of tungsten and nickel was formed, $WNiO_4$ (Figure 3a) and no discrete nickel metal or nickel oxide phases were observed. Cobalt was observed to exist as mixed phases of cobalt oxide and cobalt metal in the WO_3 films (Figure 3b). Copper and zinc were incorporated into the WO_3 in a similar fashion as cobalt.

Figure 4 shows the voltammogram of Pt−W−peroxo electrolyte (before deposition). In the case of low Pt concentration (below 5%), the voltammogram is nearly identical to that of the pure tungsten electrolyte. At high Pt concentrations, however, the shape is similar to that of the pure Pt electrolyte. When comparing XRD data from the film deposited from 15% Pt electrolyte and that from the 50% solution, we found that for lower concentrations of Pt, both Pt metal and tungsten oxide were formed. In the case of high Pt concentration, however, only crystalline Pt metal is observed with no evidence of crystalline tungsten oxide;

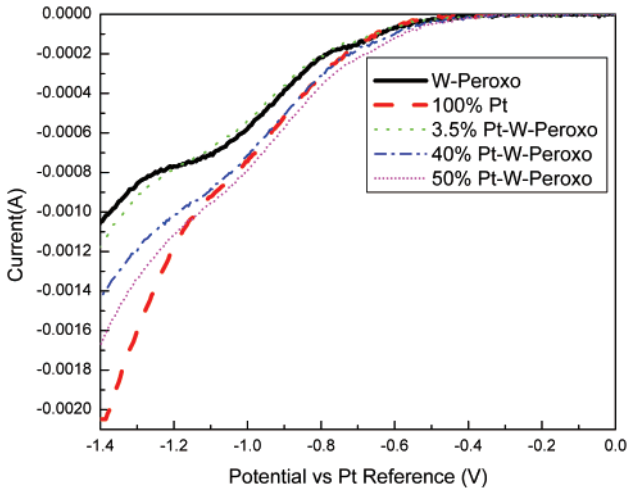

Figure 4. Deposition voltammogram of Pt−W−peroxo mixture as a function of Pt concentration.

similar results were found with Ru. Thus, when either Pt or Ru was an additive, only metal phases were distinctly observed in WO_3 films even after 600 °C calcination (Figure 3c). These observations for tungsten are in contrast to findings by Zhitomirsky et al.[23,24] in titanium dioxide, where a RuO_2−TiO_2 mixed oxide was synthesized by cathodic electrodeposition using an aqueous $RuCl_3$ and Ti peroxo mixture and calcination above 400 °C. In this system, no phase separation was noted and the authors reportedly could control the composition between the two oxides.

SEM images of Pt-doped WO_3 films are shown in Figure 5 for both low and high concentrations of Pt in the electrolyte. There are no discrete features observed that would suggest phase separation in materials deposited from low Pt concentrations (Figure 5a), whereas large distinct clusters of platinum particles (200−1000 nm) were easily seen on the tungsten oxide surface for the films synthesized from high Pt concentration electrolyte (Figure 5b). The thickness of the film was approximately 1.5−2.5 μm (Figure 5c), depending on the deposition conditions. The film compositions determined by EDX for Ni/WO_3 and Pt/WO_3 are plotted in Figure 6. As expected, with increasing concentration of additive metal ions in solution, the atomic fraction of the new substituent increased for both Ni/W and Pt/W in the film deposited. The Pt fraction showed a greater percentage increase with concentration than the Ni.

From structural and morphological evaluation, the addition of metal salts to the tungsten-based electrolyte gave rise to three distinguishable oxide groups: (1) mixed-metal oxide [Ni], (2) metal−metal oxide composites [Co, Cu, Zn], and (3) metal-doped tungsten oxide [Pt, Ru, Rh, Pd, Ag]. Whereas the peroxo-stabilized tungsten is deposited as an oxide, we speculate that the metal cations from the salts are deposited as metal, and subsequently, several are at least partially oxidized at elevated temperature where noble metals remain metallic.

The photoelectrochemical response of tungsten oxide is shown in Figure 7a. Tungsten oxide shows n-type semiconductor behavior and, under illumination, a zero bias photocurrent of 1.6 μA/cm^2 and a photocurrent of 8.5 μA/cm^2 at 1 V bias. Figure 7b shows the change of zero bias

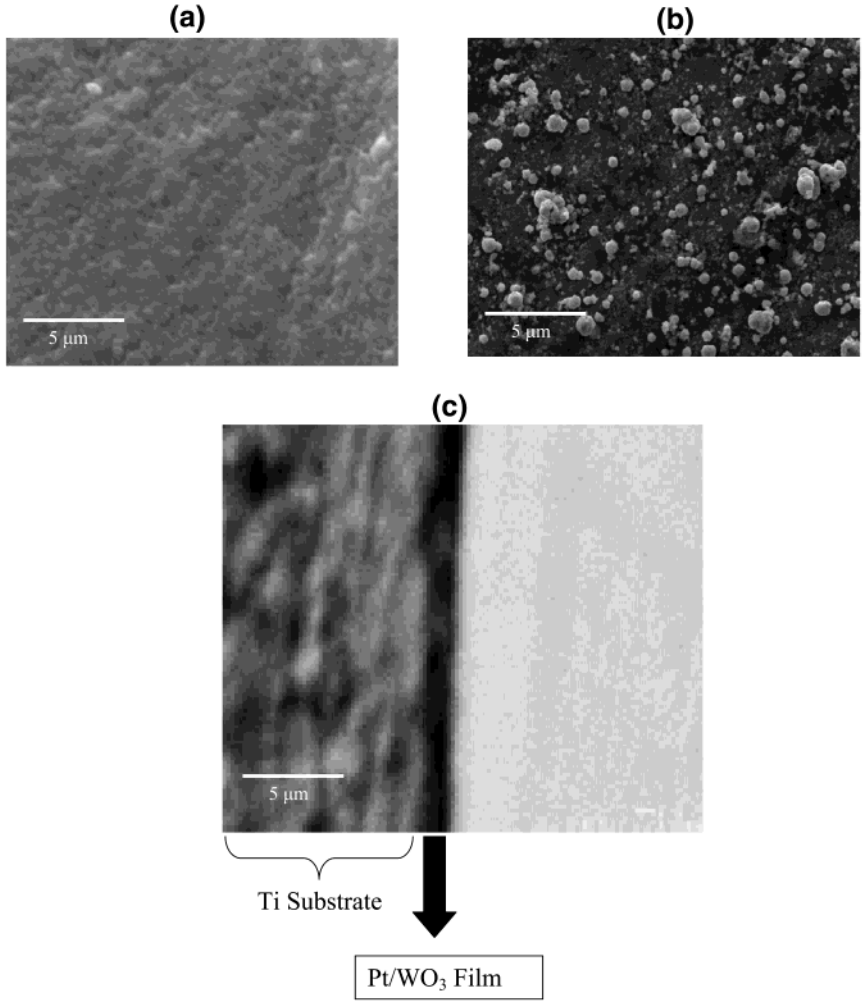

Figure 5. Scanning electron micrographs of electrodeposited Pt/WO_3 films: (a) synthesized from 3% Pt electrolyte; (b) synthesized from 50% Pt electrolyte; (c) cross-sectional view.

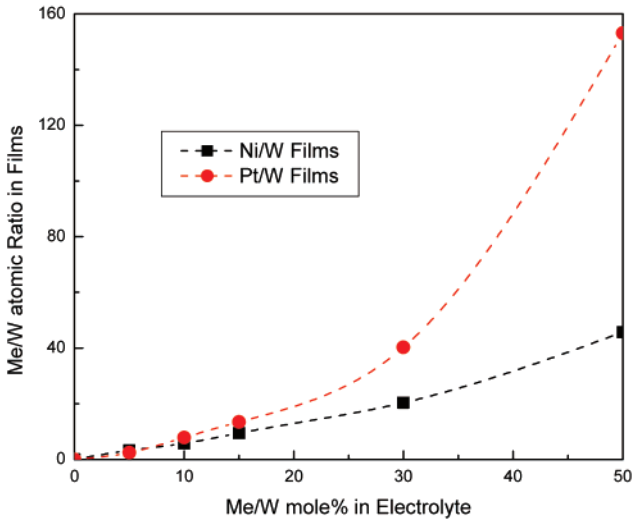

Figure 6. EDS measured atomic ratios of dopant to host (Ni/W and Pt/W) in films deposited at varied Ni or Pt salt concentrations. Dashed lines were added to guide the eye.

photocurrent with respect to calcination temperature. The as-synthesized film was amorphous and showed no photoresponse; however, with calcination there was an increase in photoactivity, presumably due to increased crystallinity and decreased defect density. This result was shown in previous work,[25] which also reported that bandgaps of tungsten oxide can be decreased by crystallization from 3.1 to 2.8 eV.

Automated photoelectrochemical screening of the libraries (libraries A and B) was performed. Figure 8 shows the photocurrents at zero bias obtained from libraries A and B. For the undoped tungsten oxide films (10 samples in both libraries A and B), a value of 1.6 ± 0.05 $\mu A/cm^2$ was observed. Substitution of KNO_3 and $HClO_4$ for acetate shows no significant change in the measured photocurrent, consistent with water (not acetate) oxidation at the photoanode. For zero bias photocurrent within the same row (same dopant at different concentrations) in library A, each dopant showed a different trend. Overall, addition of Ni showed the largest increase of the six dopants investigated; however, Co and Cu showed similar trends toward improved performance. Samples deposited from 5% to 15% of Ni concentrations showed nearly twice the photoresponse, 2.94 $\mu A/cm^2$, compared to the undoped control. There is a clear maximum at approximately 5 atomic percent, indicating that the improvement is not due to a separate NiO phase. This represents, for the broadband illumination spectrum, an IPCE (incident photon conversion efficiency) of 0.27%. Considering that only approximately 10% of the incident photon flux was of energy greater than or equal to the bandgap of WO_3, the internal quantum efficiency is expected to be greater than

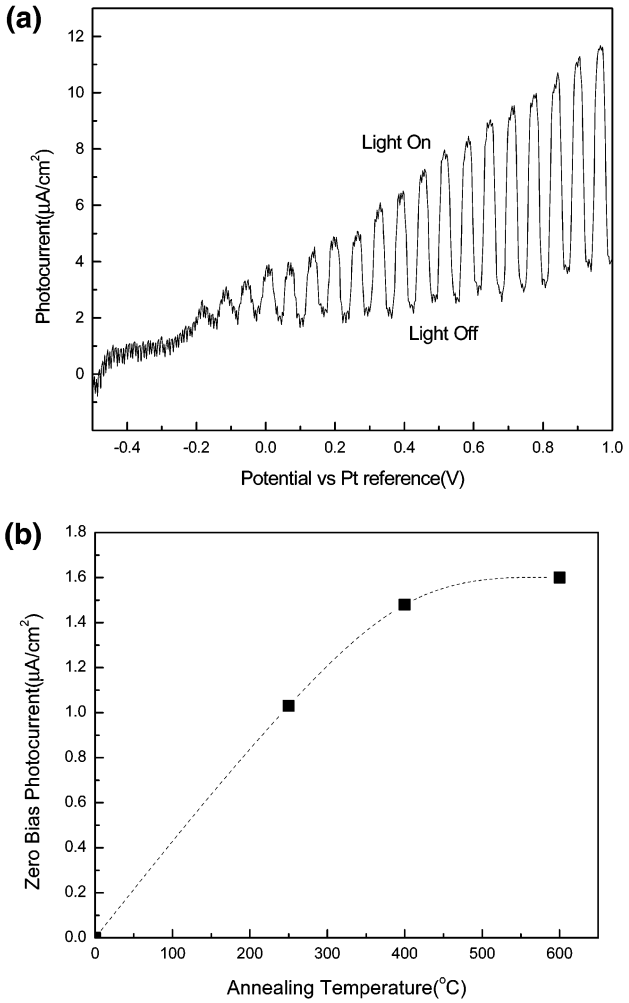

Figure 7. (a) Potentiodynamic scans under chopped illumination (2.25 mW/cm^2) for tungsten oxides and (b) zero bias photocurrent of tungsten oxide as a function of calcination temperature. Dashed lines were added to guide the eye.

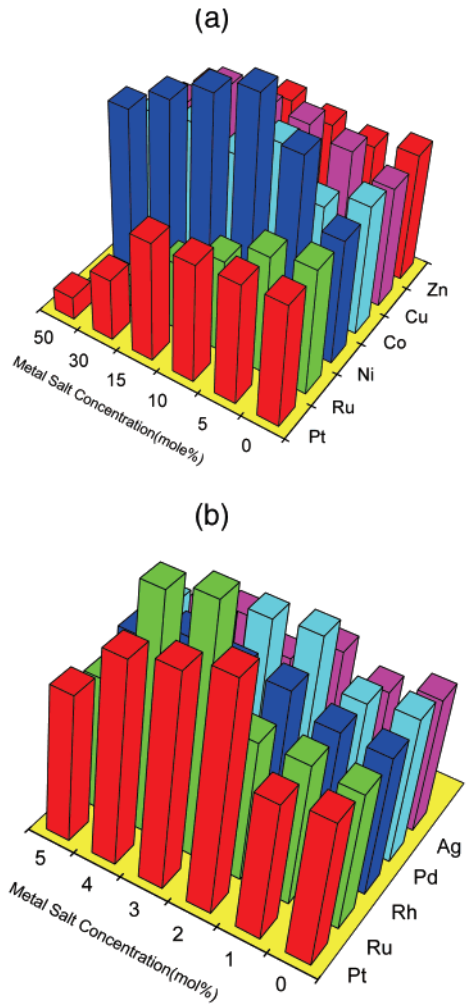

Figure 8. Zero bias photocurrent of (a) metal-doped tungsten oxide in library A and (b) noble metal doped tungsten oxides in library B.

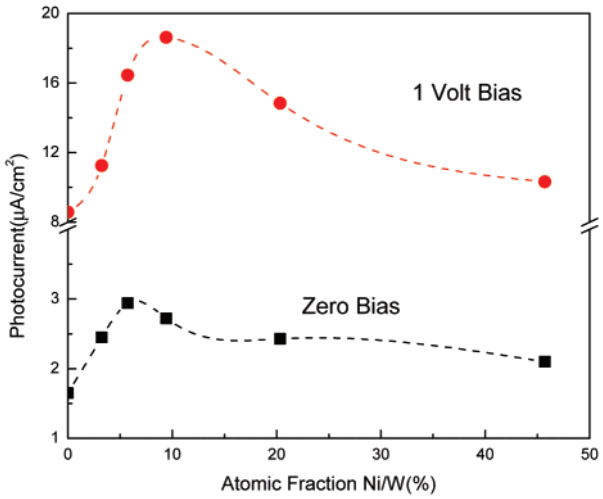

Figure 9. Photocurrents in 0.1 M sodium acetate solution at zero bias and 1 V bias for Ni-doped tungsten oxide as a function of Ni content. Dashed lines were added to guide the eye.

2.7%. The results in both Figures 6 and 8 were reproduced with negligible error in two additional libraries prepared identically.

Figure 9 shows photocurrent at 0 and 1 V bias for Ni/WO_3 (fourth row in library A) during illumination with a chopped light source in a 0.1 M sodium acetate solution. A trend in photoresponse as a function of nickel content was clearly observed. The photoresponse increased and reached a maximum when Ni content in the film was from 5 to 10 atomic percent and then decreased as the concentration of Ni content increased. Nickel is expected to exist as Ni^{2+} and, like W^{6+}, favors octahedral coordination. As a direct substituent for W, Ni^{2+} in the composite $WNiO_4$ would give rise to increased donor majority carriers and higher conductivity. It is believed that the increased photoactivity in the composite is a result of a combination of increased absorption and increased conductivity. When large amounts of nickel were added, however, phase-separated NiO was observed and is believed to decrease the photoresponse by trapping carriers at the phase boundaries. Maximum photoresponse was observed when 10% or 15% Ni salt concentrations were used (5−10 atomic percent in film). For Cu, Co, and Zn, the photoresponse was nearly independent of dopant concentration. When we used metal nitrates (Ni, Cu, Co) as precursors instead of metal chlorides, the performance trends were identical (not shown), indicating that the improved photoactivity is independent of the specific precursor.

For Ru and Pt, the zero bias photocurrent decreased as a function of dopant concentration (from 5 to 50 mol % in

library A). Phase separation was observed by SEM/EDX between WO_3 and the metal dopants at large concentrations of Pt or Ru. Such materials would not be expected to be photoactive because of recombination at the metal−semiconductor interfaces. The zero bias photocurrent of each film in library B is shown in Figure 7b. For Rh, Pd, and Ag, there is negligible change in photoresponse for the range of dopant concentrations studied. A large increase in photoactivity was observed for moderately low concentrations of Pt or Ru. Previous work by Chen et al.[26,27] reported that Pt-doped WO_3 was a very effective electrocatalyst for oxidation of low molecular weight compounds, not a photocatalyst. In that case, the atomic ratio of Pt to W was very high (approximately 1:1). Pt metal acts as an active site for the reaction, while the tungsten oxide supports and disperses Pt. Our results indicate that materials with a large atomic ratio of platinum to tungsten tend to be photoinactive, although it is confirmed that platinum particles were well dispersed on the surface of tungsten oxide. Photoactive materials could be obtained only when small amounts of highly dispersed platinum were added. The requirements for an electrocatalyst are very different from those for a photocatalyst. We clearly observed that platinum exists in metallic form. The mole fraction of Pt in Pt/WO_3 films shows a strong dependence on concentration of Pt in electrolyte. Interestingly, there is no tungsten oxide peak in the case of high Pt concentration, although the existence of tungsten was confirmed by SEM/EDX. Therefore, we can conclude that high concentrations of platinum can inhibit the deposition and crystallization of WO_3, resulting in a photoinactive material.

4. Conclusion

Combinatorial libraries of diverse metal-doped tungsten oxides were rapidly synthesized and screened with high-throughput photoelectrochemical systems. Tungsten oxide showed typical n-type behavior, and its crystallinity and photoactivity strongly depended on calcination temperature. Electrochemical deposition of the peroxo-stabilized tungsten and several metal cations gave rise to three distinguishable oxide groups: (1) mixed-metal oxides [Ni], (2) metal-doped tungsten oxides [Pt, Ru, Rh, Pd, Ag], and (3) metal−metal oxide composites [Co, Cu, Zn]. The semiconducting oxides typically showed n-type behavior.

By introduction of various dopants into WO_3, changes in photoactivity were observed. Nickel was found to be the most effective photoelectrochemical dopant for tungsten oxide, probably by increasing the conductivity and decreasing charge carrier recombination in the WO_3. Pt and Ru, at concentrations above 5%, inhibited the crystallization of WO_3, resulting in decrease of photoactivity. Concentrations of Pt and Ru below 5% were found to be effective for increasing the photoactivity of tungsten oxide probably by forming well-dispersed metallic clusters that reduced the overpotential for oxidation.

Acknowledgment. Major funding was provided by the Hydrogen Program of the Department of Energy (DOE Grant No. DE-FC36-01G011092) and the Cycad Group (Santa Barbara, CA). Partial funding and facilities were provided by the NSF-MRSEC funded Materials Research Laboratory (UCSB) and the California Energy Commission (CEC Grant No. 51539A/99-36). The authors appreciate the technical assistance of Anna Ivanovskaya.

References and Notes

(1) Yao, J. N.; Chen, D.; Fujishima, A. *J. Electroanal. Chem.* **1996**, *406*, 223−226.
(2) Granqvist, C. G. *Sol. Energy Mater. Sol. Cells* **2000**, *60*, 201−262.
(3) Hutchins, M. G.; Kamel, N. A.; El-Kardy, W.; Ramadan, A. A.; Abdel-Hady, K. *Phys. Status Solidi. A* **1999**, *175*, 991−1002.
(4) Solis, J. L.; Hoel, A.; Lantto, V.; Granqvist, C. G. *J. Appl. Phys.* **2001**, *89*, 2727−2732.
(5) Azens, A.; Stjerma, B.; Granqvist, C. G.; Gabrusenoks, J.; Lusis, A. *Appl. Phys. Lett.* **1994**, *65*, 1998−2000.
(6) Le Bellac, D.; Azens, A.; Granqvist, C. G. *Appl. Phys. Lett.* **1995**, *66*, 1715−1716.
(7) Kulesza, P. J.; Faulkner, L. R. *J. Am. Chem. Soc.* **1988**, *110*, 4905−4913.
(8) Su, L.; Zhang, L.; Fang, J.; Xu, M.; Lu, Z. *Sol. Energy Mater. Solar Cells* **1999**, *58*, 133−140.
(9) Shen, P. K.; Tseung, C. C. *J. Mater. Chem.* **1992**, *2* (11) 1141−1147.
(10) Meulenkamp, E. A. *J. Electrochem. Soc.* **1997**, *144*, 1664−1671.
(11) Shen, P. K.; Bokhari, J. S.; Tseung, A. C. C. *J. Electrochem. Soc.* **1991**, *138*, 2778−2783.
(12) Lee, S.-H.; Park, Y.-S.; Joo, S.-K. *Solid State Ionics* **1998**, *109*, 303−310.
(13) Hanak, J. J. *J. Mater. Sci.* **1970**, *5*, 964−971.
(14) McFarland, E. W.; Weinberg, W. H. *J. Mater. Technol.* **1998**, *13* (3), 107−120.
(15) Hanak, J. J.; Gittleman, J. I.; Pellican, J. P.; Bozowski, S. *Phys. Lett.* **1969**, *30A*, 201−202.
(16) Hanak, J. J.; Gittleman, J. I. *Physica* **1971**, *55*, 555−561.
(17) Danielson, E.; Devenney, M.; Giaquinta, D. M.; Golden, J. H.; Haushalter, R. C.; McFarland, E. W.; Poojary, D. M.; Reaves, C. M.; Weinberg, W. H.; Wu, X. D. *Science* **1998**, *279*, 837−839.
(18) Danielson, E.; Golden, J. H.; McFarland, E. W.; Reaves, C. M.; Weinberg, W. H.; Wu, X. D. *Nature* **1997**, *389*, 944−948.
(19) Cong, P.; Doolen, R. D.; Fan, Q.; Giaquinta, D. M.; Guan, S.; McFarland, E. W.; Poojary, D. M.; Self, K.; Turner, H. W.; Weinberg, W. H. *Angew. Chem., Int. Ed.* **1999**, *38* (4), 484−488.
(20) Reddington, E.; Sapienza, A.; Gurau, B.; Viswanathan, R.; Sarangapani, S.; Smothkin, E. S.; Mallouk, T. E. *Science* **1998**, *280*, 1735−1737.
(21) Brandli, C.; Jaramillo, T. F.; Ivanovskaya, A.; McFarland, E. W. *Electrochim. Acta* **2001**, *47*, 553−557.
(22) McFarland, E. W.; Baeck, S. H.; Brandli, C.; Ivanovskaya, A.; Jaramillo, T. F. *Proc. Can. Hydrol. Conf., 11th*, in press.
(23) Zhitomirsky, I. *Mater. Lett.* **1998**, *33*, 305−310.
(24) Zhitomirsky, I.; Gal-Or, L. *Mater. Lett.* **1997**, *31*, 155−159.
(25) Miyauchi, M.; Nakajima, A.; Hashimoto, K.; Watanabe, T. *Adv. Mater.* **2000**, *12* (24), 1923−1927.
(26) Chen, Y.; Chen, K. Y.; Tseung, A. C. C. *J. Electroanal. Chem.* **1999**, *471*, 151−155.
(27) Shen, P. K.; Chen, K. Y.; Tseung, A. C. C. *J. Electroanal. Chem.* **1995**, *389*, 223−225.

CC020014W